

Diffusion tensor imaging of white matter in the superior temporal gyrus and temporal stem in autism[☆]

Jee Eun Lee^a, Erin D. Bigler^{e,f,g,k}, Andrew L. Alexander^{a,b,c,*}, Mariana Lazar^a,
Molly B. DuBrayⁱ, Moo K. Chung^{a,d}, Michael Johnson^f, Jubel Morgan^f,
Judith N. Miller^f, William M. McMahon^{f,k}, Jeffrey Lu^h,
Eun-Kee Jeong^{g,j}, Janet E. Lainhart^{f,i,j,k}

^a Waisman Laboratory for Brain Imaging and Behavior, Waisman Center, Madison, WI, United States

^b Department of Medical Physics, University of Wisconsin, Madison, WI, United States

^c Department of Psychiatry, University of Wisconsin, Madison, WI, United States

^d Department of Biostatistics and Medical Informatics, University of Wisconsin, Madison, WI, United States

^e Department of Psychology, Brigham Young University, Provo, UT, United States

^f Department of Psychiatry, University of Utah, Salt Lake City, UT, United States

^g Department of Radiology, University of Utah, Salt Lake City, UT, United States

^h Department of Anesthesiology, University of Utah, Salt Lake City, UT, United States

ⁱ Neuroscience Program, University of Utah, Salt Lake City, UT, United States

^j Center for Advanced Imaging Research, Salt Lake City, UT, United States

^k The Brain Institute at The University of Utah, Salt Lake City, UT, United States

Received 23 April 2007; received in revised form 2 July 2007; accepted 24 July 2007

Abstract

Recent MRI studies have indicated that regions of the temporal lobe including the superior temporal gyrus (STG) and the temporal stem (TS) appear to be abnormal in autism. In this study, diffusion tensor imaging (DTI) measurements of white matter in the STG and the TS were compared in 43 autism and 34 control subjects. DTI measures of mean diffusivity, fractional anisotropy, axial diffusivity, and radial diffusivity were compared between groups. In all regions, fractional anisotropy was significantly decreased and both mean diffusivity and radial diffusivity were significantly increased in the autism group. These results suggest that white matter microstructure in autism is abnormal in these temporal lobe regions, which is consistent with theories of aberrant brain connectivity in autism.

© 2007 Published by Elsevier Ireland Ltd.

Keywords: Autism; Diffusion tensor imaging; Superior temporal gyrus; Temporal stem; White matter; Anisotropy; Diffusivity; Magnetic resonance imaging

A prevalent hypothesis is that brain connectivity in autism is aberrant (e.g. [6,11]). Regional abnormalities in cerebral white matter (WM) can result in impaired brain connectivity. Conse-

quently, evidence of abnormal white matter would significantly strengthen the case for the disconnectivity hypothesis in autism.

Traditionally, the superior temporal gyrus (STG) has been defined primarily by its role in auditory processing [19,22]. Contemporary cognitive neuroscience views the STG as equally important in social cognition, regulation of behavior, and neural mechanisms of imitation [1,16]. As such, the role of the STG in autism has become the focus of several structural and functional neuroimaging studies [9,13,21]. Despite the functional abnormalities associated with the autistic temporal lobe, studies of overall STG volumetric differences between autism and controls have yielded inconsistent findings. One volumetric study reported smaller left STG volumes in autism [24], whereas other studies have reported no volumetric differences

Abbreviations: Da, axial (parallel) diffusivity; Dr, radial (perpendicular) diffusivity; DTI, diffusion tensor imaging; FA, fractional anisotropy; MD, mean diffusivity; STG, superior temporal gyrus; TS, temporal stem; WM, white matter

[☆] This study was approved by the following Institutional Review Boards: University of Utah IRB: IRB 00010391 (PI: Lainhart, approval 9 May 2007). University of Wisconsin Health Sciences IRB: H-2003-0548 (PI: Alexander, approval 12 March 2007).

* Corresponding author at: Waisman Laboratory for Brain Imaging and Behavior, Waisman Center, 1500 Highland Avenue, Madison, WI 53705, United States. Tel.: +1 608 265 8233.

E-mail address: alalexander2@wisc.edu (A.L. Alexander).

[7,8]. Since autism has features of both impaired communication and social processing [4], investigation of the white matter projections to the STG may help to understand abnormal STG function in autism [21].

Major afferent and efferent connections of the temporal lobe (including STG) enter and exit via the temporal stem (TS) [18]. This deep WM area bridges the temporal cortex with important limbic, thalamic, striatal, and frontal regions [18]. The temporal stem includes portions of the uncinate fasciculus and inferior occipitofrontal fasciculus. Several analyses have shown that subtle reduction in white matter volume of the TS area may occur in autism [8,20]. Volumetric reduction of the TS area may be a sign of impaired connectivity between the temporal lobe and the rest of the brain.

Diffusion tensor imaging (DTI) is a promising method for characterization of tissue microstructure in the CNS [5]. In WM, the membranes of the axons and myelin cause the apparent (radial) diffusivities of water perpendicular to the white matter tracts to be decreased relative to the (axial) diffusivities in the directions parallel to the white matter fibers. Changes in the WM microstructure (e.g., myelination, axonal density, etc.) will consequently affect the diffusion anisotropy. Thus, DTI measurements of WM in the STG and TS may be used to characterize microstructural abnormalities in the autistic temporal lobe that may be undetectable at the volumetric level. Two DTI studies of the autistic temporal lobe reported reduced fractional anisotropy (FA) bilaterally adjacent to the superior temporal sulcus [3] and in deeper WM in the right posterior limb of the internal capsule [17]. These studies suggest abnormalities in the superior and deeper temporal white matter microstructure and warrant further investigation. Recent DTI studies have also demonstrated microstructural abnormalities in the corpus callosum in autism [2]. In the current study, the microstructural properties of temporal lobe WM in regions of the STG and TS in autism were examined using the DTI measures of mean diffusivity (MD), fractional anisotropy (FA), radial diffusivity (D_r), and axial diffusivity (D_a). Measurements were compared between subjects with high functioning autism and controls.

Forty-three subjects with a lifetime-diagnosis of autism-spectrum disorder (38 autism, 5 PDD-NOS) were compared to 34 control subjects. Informed consent and assent were obtained for all subjects prior to participation. All aspects of the study had received IRB approval. All subjects were males, non-mentally retarded ($IQ > 85$), from the greater Salt Lake City, Utah region, and the two groups were matched in terms of age (autism: 16.2 ± 6.7 with range = 7–33 years; control: 16.4 ± 6.0 with range = 8–29 years; $p = 0.89$), performance IQ (autism: 107.5 ± 13.0 ; control: 112.8 ± 12.0 ; $p = 0.07$), handedness (autism: 80.81 ± 21.7 ; control: 72.79 ± 29.0 ; $p = 0.17$), and head circumference (autism: 56.6 ± 2.3 ; control: 56.1 ± 2.0 ; $p = 0.34$). Head circumference was used as a matching variable to control for the increased rate of macrocephaly in autism. A volumetric study showed that white matter volume differences between autism and control subjects were non-significant when the effect of the increased rate of macrocephaly was controlled [8]. All subject testing and imaging experiments were performed

at the University of Utah. Image analysis was performed at the University of Wisconsin.

Autism and control (typically developing) subjects were recruited during a 3-year period (2002–2005) from community sources, including parent support groups, youth groups, and schools, and from clinic social skills groups as part of an ongoing longitudinal study of autism.

Autism was rigorously diagnosed, as has been described elsewhere [8], based on the Autism Diagnostic Interview-Revised (ADI-R), Autism Diagnostic Observation Schedule-Generic (ADOS-G), and DSM-IV and ICD-10 criteria. History, observation, Fragile-X gene testing, and karyotype were used to exclude medical causes of autism. None of the autism subjects had a history of seizures.

Control subjects had no history of learning, developmental, cognitive, neurological, or neuropsychiatric problems. All controls had extensive testing, including the ADOS-G, IQ, language, and psychiatric testing, to confirm that they were typically developing.

Diffusion tensor (DT) images were acquired on a Siemens Trio 3.0 Tesla MRI Scanner. Four of the children with autism were sedated by an anesthesiologist (JL) for scanning, and were continuously monitored according to American Society of Anesthesiology standards. There were no complications associated with the sedation. A wide range of other pulse sequences (T1-weighted Magnetization-Prepared Rapid Gradient-Echo (MP-RAGE), and T2-weighted Turbo Spin Echo) were collected for both clinical review and quantitative analyses although these data were not used in the current analysis. An eight-channel RF receiver coil was used to acquire the imaging data. DTI was performed using a product single-shot, echo planar imaging pulse sequence with dual-refocusing and bipolar diffusion-weighting gradients to reduce eddy currents. Parallel imaging with SENSE (Sensitivity Encoding) was performed using a reduction factor of 2 to reduce image distortion. The in-plane resolution was 2 mm isotropic (field of view = 256 mm; matrix = 128×128). A single ($b = 0$) reference image volume and 12 diffusion-weighted image volumes with non-collinear diffusion encoding directions and diffusion weighting $b = 1000 \text{ s/mm}^2$ were obtained. Each image volume covered the cerebrum and cerebellum with fifty 2.5 mm thick contiguous axial slices. Other imaging parameters were TR (repetition time) = 7000 ms, TE (echo time) = 84 ms, acquisition sampling bandwidth per pixel = 1345 Hz, and 3 averages. A field map was generated from a pair of 2D gradient echo images with different echo times (TE1 = 7 ms, TE2 = 10 ms).

All of the image processing was performed using custom software and command-line scripts developed in-house. Misregistration effects from eddy currents and head movements were first corrected using affine registration software (AIR—<http://bishopw.loni.ucla.edu/AIR5/>). Spatial distortions in the EPI data from magnetic field (B_0) inhomogeneities were corrected using field map correction software scripts with ‘prelude’ and ‘fugue’ from the FMRIB software library (<http://www.fmrib.ox.ac.uk/fsl/>). Corrected images were interpolated to 2 mm isotropic voxels and diffusion tensor maps were subsequently estimated. Maps of the diffusion tensor eigenval-

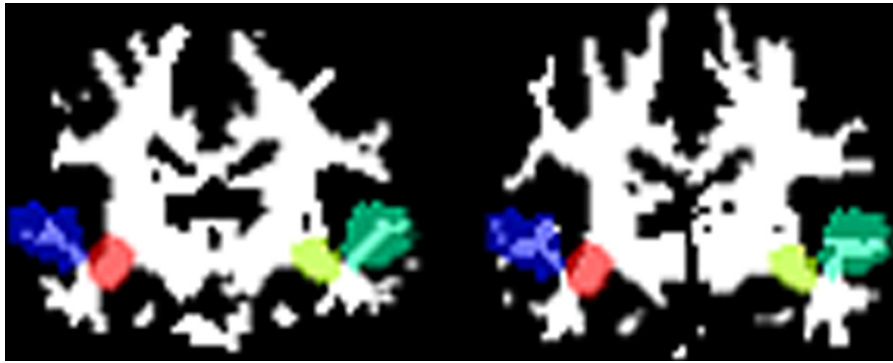


Fig. 1. Example ROI overlays on the segmented WM regions on affine normalized image data for both control (left) and autistic (right) subjects. The coronal cross-sections are the segmented white matter maps. The STG–WM regions are labeled in blue (right) and green (left), and the TS regions are labeled in red (right) and yellow (left). Only voxels that intersect both the ROI template and WM mask were used in the analyses.

ues ($\lambda_1, \lambda_2, \lambda_3$), MD, FA, $D_a (= \lambda_1)$, and $D_r (= (\lambda_2 + \lambda_3)/2)$ were generated.

In this study, WM regions of interest identifying the STG–WM and TS were extracted in two steps. First, cerebral WM was segmented using the mFAST algorithm in the FMRIB software library with maps of the major and minor eigenvalues (λ_1 and λ_3 , respectively) as the inputs. This combination of eigenvalues appeared to yield the most robust white matter segmentation (compared with any single eigenvalue, MD, FA or any other combination). In each subject, voxels with MD values two standard deviations from the average MD in the total WM were excluded from the WM segmentation as these were likely contaminated with CSF. The segmented WM volume masks were then co-registered to a custom WM template. Regions in the STG and TS were then identified on the mask average and regions were labeled on the WM template. The right and left STG–WM and TS region templates were then transformed back to the native space of each subject's DTI data and the regions were overlaid on the segmented DTI maps for that subject. Example overlays are illustrated in Fig. 1. This provided a semi-automated method for labeling these regions on each subject in the native space. Mean values of MD, FA, D_a and D_r were extracted in each region. Manual inspection of the automated STG–WM and TS labeling demonstrated consistent extraction of these regions.

DTI measurements of FA, MD, D_a and D_r were compared using a one-way ANCOVA (using custom Matlab software and verified using SPSS version 14.0) with group as the independent variable, DTI measurements as the dependent variables, and age as the covariate. Age was covaried because DTI measures have age-dependence. The four regions—right and left STG–WM and TS were analyzed independently. Since four regions were evaluated, the effects of multiple comparisons were compensated using a Bonferroni correction, such that results were thresholded at an uncorrected $p < 0.013$. All reported p -values are uncorrected.

Statistical analyses for the study are summarized in Table 1, including the summary statistics (means and standard deviations of the DTI measures in both autism and controls), group comparisons using ANCOVA, and the correlation coefficients (R) of the regional measures with age over all subjects. In all regions,

D_r was significantly elevated in autism relative to controls. MD was significantly higher in autism for the right TS and right STG–WM, and in the left STG–WM. FA measurements were significantly lower in autism for all regions. Significant group differences in D_a were observed in right STG–WM. The regional volumes were not significantly different between groups.

In general, both MD and D_r decreased with age for both groups (see Fig. 2a and Table 1). FA appeared to increase with age for controls whereas very little age-related changes were detected for the autism group (see Fig. 2b). However, only the right STG–WM appeared to demonstrate significant age \times group interactions for FA ($F = 15.02$; $p = 0.0002$). Conversely, D_a appeared to decrease with age for the autism group, whereas D_a showed minimal age-related changes in controls except in the left STG–WM. However, the age \times group interactions for D_a were again only significant for the right STG–WM ($F = 9.52$; $p = 0.0029$). None of the other regions demonstrated significant age \times group interactions ($F < 3.85$). The age \times group interactions for FA and D_a in the right STG–WM mean that the results will depend upon the age composition of the subjects being studied for these measures. Plots of all DTI measures versus age for all regions are available as on-line [supplementary material](#).

The potential effects of medication on the DTI measurements were also investigated. Twenty-six (60%) of the autism subjects were taking at least one psychotropic medication and 38% were taking multiple medications. Seventy-three percent of the autism subjects were taking SSRI's, 35% stimulants, 11% valproic acid, and 7% atypical neuroleptics. There were no significant differences in either the mean age or any of the DTI measures in autism subjects taking psychotropic medications versus those not on medications. The significant regions were the same when autism subjects were split into the medication and non-medication groups except the MD in the left TS dropped below significance for the autism medication subgroup.

Four of the younger subjects with autism (ages 7–10) were scanned with sedation. We compared the DTI measurements of the autism subjects with sedation ($n = 4$) against those from the autism subjects without sedation in the same age range ($n = 6$). Although the MD and D_r measures were generally larger in the sedated group, the differences were nearly significant only

Table 1
Group comparisons of anisotropy and diffusivities

	Autism (<i>n</i> = 43)		Control (<i>n</i> = 34)		Age correlation		ANCOVA (w/age) group comparison	
	Mean	S.D.	Mean	S.D.	<i>R</i>	<i>p</i>	<i>F</i>	<i>p</i> (uncorrected)
Mean diffusivity (10^{-3} mm ² /s)								
Left temporal stem	0.875	0.024	0.866	0.023	−0.30	0.007*	3.6	0.063
Right temporal stem	0.886	0.025	0.867	0.021	−0.37	0.001*	14.6	0.000*
Left STG–WM	0.836	0.033	0.818	0.033	−0.54	0.000*	7.9	0.006*
Right STG–WM	0.830	0.033	0.807	0.028	−0.59	0.000*	16.4	0.000*
Fractional anisotropy								
Left temporal stem	0.400	0.021	0.415	0.023	0.24	0.039	9.1	0.004*
Right temporal stem	0.392	0.027	0.410	0.029	0.22	0.054	8.2	0.005*
Left STG–WM	0.314	0.022	0.331	0.021	0.30	0.009*	13.9	0.000*
Right STG–WM	0.311	0.018	0.322	0.026	0.40	0.000*	6.8	0.011*
Axial diffusivity (10^{-3} mm ² /s)								
Left temporal stem	1.277	0.032	1.279	0.035	−0.14	0.228	0.1	0.776
Right temporal stem	1.283	0.027	1.277	0.031	−0.19	0.096	1.0	0.327
Left STG–WM	1.116	0.042	1.108	0.041	−0.49	0.000*	0.7	0.402
Right STG–WM	1.107	0.042	1.086	0.032	−0.45	0.000*	7.8	0.007*
Radial diffusivity (10^{-3} mm ² /s)								
Left temporal stem	0.675	0.028	0.659	0.027	−0.30	0.008*	6.9	0.011*
Right temporal stem	0.688	0.034	0.662	0.031	−0.32	0.004*	12.7	0.001*
Left STG–WM	0.697	0.034	0.673	0.033	−0.50	0.000*	12.6	0.001*
Right STG–WM	0.691	0.032	0.668	0.032	−0.58	0.000*	16.2	0.000*
Volume (voxels)								
Left temporal stem	245.8	31.8	242.6	34.3	0.32	0.005*	0.2	0.639
Right temporal stem	235.6	31.5	239.2	35.7	0.17	0.151	0.2	0.649
Left STG–WM	321.3	115.2	371.2	110.3	0.42	0.000*	4.3	0.042
Right STG–WM	343.1	96.2	394.1	127.8	0.56	0.000*	5.6	0.020

* Statistically significant at the thresholded uncorrected $p < 0.013$, determined by Bonferroni correction for multiple comparisons.

in right STG–WM for MD ($p = 0.018$), Da ($p = 0.03$), and Dr ($p = 0.057$). When the four sedated subjects were removed from the overall ANCOVA, the regions with significant differences were similar to those in Table 1 except for Dr in the left TS was not quite significant ($F = 4.42$; $p = 0.039$).

In the current study, we implemented a semi-automated ROI approach for obtaining DTI measures in specific temporal lobe regions. Since the ROIs were applied to segmented WM data, the contamination from gray matter and CSF was minimal. Also, the regions were large enough to accommodate errors in mis-registration.

The current findings demonstrated DTI differences in the WM of the STG and TS, implicating dissimilarities in microstructural organization of these temporal lobe regions in autism compared to controls. Since these are critical pathways involved in language and social cognition, WM abnormalities within these regions may contribute to the neurobehavioral features observed in autism. The radial diffusivity, Dr, was consistently elevated in autism. The differences in Dr appear to be the primary cause for changes in MD and FA measures. This observation of increased Dr was consistent with DTI measurements of the corpus callosum in autism [2]. Recent studies in a mouse model of dysmyelination have suggested that increases in the radial diffusivity are related to myelination [23]. However, it was not clear if differences in myelination were the primary mechanism for the DTI changes reported here. Changes in axonal density, organization or gliosis might also affect the

radial diffusivity. Psychotropic medication use did not appear to have a major effect on the findings.

It is interesting that the MD and Dr measurements appear to be quite elevated in autism for the youngest subjects (ages 7–13, for example, see Fig. 2a for Dr in right TS). Whether these increased diffusivities in mid-childhood are indicative of an aberrant developmental trajectory is not clear. Currently, we are performing a longitudinal DTI study on these subjects, which will be better for assessing differences in the developmental trajectories between groups. Sedation for scanning of 4 young subjects did not appear to have a major effect on the overall results.

In this study, it was hypothesized that the microstructural features of specific WM regions in the temporal lobe are affected in autism, and the data were consistent with the prediction. However, it is likely that other brain regions in autism will also show WM abnormalities. Indeed, the corpus callosum in these same subjects were abnormal [2] and a small voxel-based analysis study by Barnea-Goraly et al. [3] suggested diffuse WM differences though not specifically in the TS and STG. Future studies will investigate whether other WM regions are likewise affected. Finally, it is also possible that gray matter regions are also affected in autism; however, characterization of cortical gray matter with DTI is extremely challenging because it is relatively narrow and adjacent to CSF.

The results from this study demonstrate that WM regions of the temporal lobe – the STG and TS – appear to be abnormal in

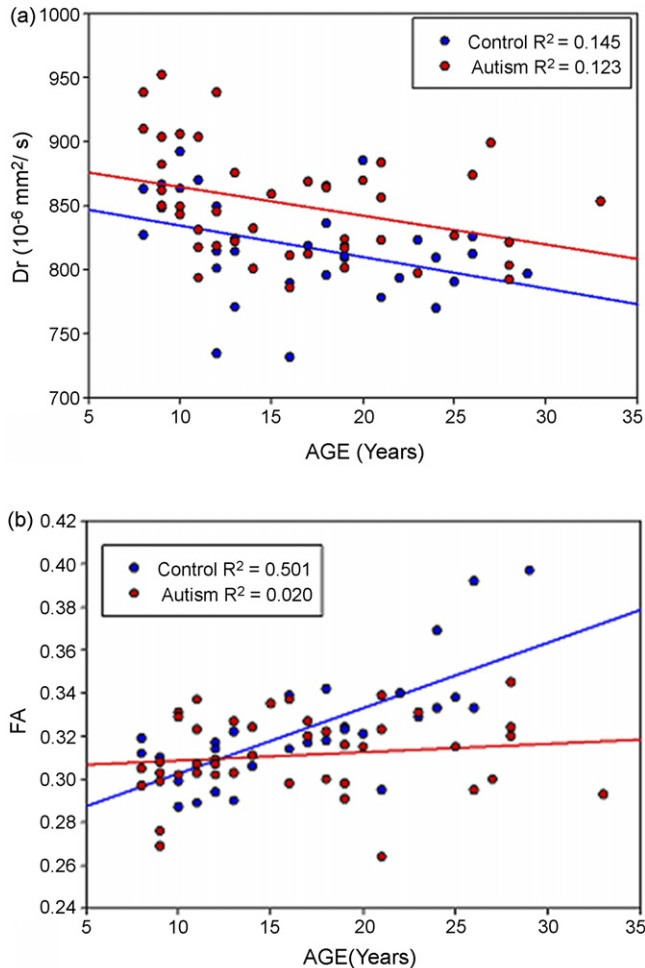


Fig. 2. (a) Measurements of Dr vs. age in right TS. The plot shows a similar decline with age for both groups and an increased Dr in the autism group. The results for the other regions were similar. (b) Measurements of FA vs. age in right STG–WM. FA appears to increase with age for the controls; however, the autistic subjects demonstrated minimal changes with age. The age-dependence was significantly different between groups. Similar trends were observed for the other regions; however, the group difference was not significant.

subjects with autism. These regions are critical to language and social function, which are affected in autism. These findings add to functional neuroimaging studies demonstrating abnormalities of the STG in autism [10,12], and support the hypothesis that autism involves abnormal brain connectivity [14,15]. Future studies are necessary to determine how specifically related these WM abnormalities are to language and social impairments.

Acknowledgments

This work was supported by the NIH grants HD35476, NIMH 62015, NIDA15879, the NICHD/NIDCD Collaborative Programs of Excellence in Autism (CPEA), the NIH Mental Retardation/Developmental Disabilities Research Center (Waisman Center), the Autism Society of Southwestern Wisconsin, and the National Alliance for Research in Schizophrenia and Affective Disorders (NARSAD). We thank Brad Wright and the PIs and staff of the Utah Autism Research Program: Dr.

Hilary Coon, Dr. Robert Fujinami, Tami Elsner, Lori Krasny, Megan Farley, Heidi Block, Lindsey Warner, Barbara Young, Tracy Abildskov, and JoAnn Petrie. We also thank Melody Johnson, Henry Buswell, and the rest of the UCAIR staff. We express our sincere gratitude to the children and adults who participated in this study and their families.

Appendix A. Supplementary data

Supplementary data associated with this article can be found, in the online version, at doi:10.1016/j.neulet.2007.07.042.

References

- [1] R. Adolphs, Cognitive neuroscience of human social behaviour, *Nat. Rev. Neurosci.* 4 (2003) 165–178.
- [2] A.L. Alexander, J.E. Lee, M. Lazar, R. Boudos, M.B. DuBray, T.R. Oakes, J.N. Miller, J. Lu, E.K. Jeong, W.M. McMahon, E.D. Bigler, J.E. Lainhart, Diffusion tensor imaging of the corpus callosum in Autism, *Neuroimage* 34 (2007) 61–73.
- [3] N. Barnea-Goraly, H. Kwon, V. Menon, S. Eliez, L. Lotspeich, A.L. Reiss, White matter structure in autism: preliminary evidence from diffusion tensor imaging, *Biol. Psychiatry* 55 (2004) 323–326.
- [4] S. Baron-Cohen, M.K. Belmonte, Autism: a window onto the development of the social and the analytic brain, *Annu. Rev. Neurosci.* 28 (2005) 109–126.
- [5] P.J. Basser, J. Mattiello, D. LeBihan, MR diffusion tensor spectroscopy and imaging, *Biophys. J.* 66 (1994) 259–267.
- [6] M.K. Belmonte, G. Allen, A. Beckel-Mitchener, L.M. Boulanger, R.A. Carper, S.J. Webb, Autism and abnormal development of brain connectivity, *J. Neurosci.* 24 (2004) 9228–9231.
- [7] E.D. Bigler, S. Mortensen, E.S. Neeley, S. Ozonoff, L. Krasny, M. Johnson, J. Lu, S.L. Provencal, W. McMahon, J.E. Lainhart, Superior temporal gyrus, language function, and autism, *Dev. Neuropsychol.* 31 (2007) 217–238.
- [8] E.D. Bigler, D.F. Tate, E.S. Neeley, L.J. Wolfson, M.J. Miller, S.A. Rice, H. Cleavinger, C. Anderson, H. Coon, S. Ozonoff, M. Johnson, E. Dinh, J. Lu, W. McMahon, J.E. Lainhart, Temporal lobe, autism, and macrocephaly, *AJNR Am. J. Neuroradiol.* 24 (2003) 2066–2076.
- [9] N. Boddaert, P. Belin, N. Chabane, J.B. Poline, C. Barthelemy, M.C. Mouren-Simeoni, F. Brunelle, Y. Samson, M. Zilbovicius, Perception of complex sounds: abnormal pattern of cortical activation in autism, *Am. J. Psychiatry* 160 (2003) 2057–2060.
- [10] N. Boddaert, N. Chabane, H. Gervais, C.D. Good, M. Bourgeois, M.H. Plumet, C. Barthelemy, M.C. Mouren, E. Artiges, Y. Samson, F. Brunelle, R.S. Frackowiak, M. Zilbovicius, Superior temporal sulcus anatomical abnormalities in childhood autism: a voxel-based morphometry MRI study, *Neuroimage* 23 (2004) 364–369.
- [11] E. Courchesne, K. Pierce, Why the frontal cortex in autism might be talking only to itself: local over-connectivity but long-distance disconnection, *Curr. Opin. Neurobiol.* 15 (2005) 225–230.
- [12] I. Gendry Meresse, M. Zilbovicius, N. Boddaert, L. Robel, A. Philippe, I. Sfaello, L. Laurier, F. Brunelle, Y. Samson, M.C. Mouren, N. Chabane, Autism severity and temporal lobe functional abnormalities, *Ann. Neurol.* 58 (2005) 466–469.
- [13] G.J. Harris, C.F. Chabris, J. Clark, T. Urban, I. Aharon, S. Steele, L. McGrath, K. Conouris, H. Tager-Flusberg, Brain activation during semantic processing in autism spectrum disorders via functional magnetic resonance imaging, *Brain Cogn.* 61 (2006) 54–68.
- [14] J. Hendry, T. DeVito, N. Gelman, M. Densmore, N. Rajakumar, W. Pavlosky, P.C. Williamson, P.M. Thompson, D.J. Drost, R. Nicolson, White matter abnormalities in autism detected through transverse relaxation time imaging, *Neuroimage* 29 (2006) 1049–1057.
- [15] M.R. Herbert, Large brains in autism: the challenge of pervasive abnormality, *Neuroscientist* 11 (2005) 417–440.

- [16] M. Iacoboni, Neural mechanisms of imitation, *Curr. Opin. Neurobiol.* 15 (2005) 632–637.
- [17] T.A. Keller, R.K. Kana, M.A. Just, A developmental study of the structural integrity of white matter in autism, *Neuroreport* 18 (2007) 23–27.
- [18] E.L. Kier, L.H. Staib, L.M. Davis, R.A. Bronen, MR imaging of the temporal stem: anatomic dissection tractography of the uncinate fasciculus, inferior occipitofrontal fasciculus, and Meyer's loop of the optic radiation, *AJNR Am. J. Neuroradiol.* 25 (2004) 677–691.
- [19] M. Meyer, T. Zaehle, V.E. Gountouna, A. Barron, L. Jancke, A. Turk, Spectro-temporal processing during speech perception involves left posterior auditory cortex, *Neuroreport* 16 (2005) 1985–1989.
- [20] E.S. Neeley, E.D. Bigler, L. Krasny, S. Ozonoff, W. McMahon, J.E. Lainhart, Quantitative temporal lobe differences: autism distinguished from controls using classification and regression tree analysis, *Brain Dev.* 29 (2007) 389–399.
- [21] K. Pelphrey, R. Adolphs, J.P. Morris, Neuroanatomical substrates of social cognition dysfunction in autism, *Ment. Retard. Dev. Disabil. Res. Rev.* 10 (2004) 259–271.
- [22] S.A. Ruschemeyer, S. Zysset, A.D. Friederici, Native and non-native reading of sentences: an fMRI experiment, *Neuroimage* 31 (2006) 354–365.
- [23] S.K. Song, S.W. Sun, M.J. Ramsbottom, C. Chang, J. Russell, A.H. Cross, Demyelination revealed through MRI as increased radial (but unchanged axial) diffusion of water, *Neuroimage* 17 (2002) 1429–1436.
- [24] G.D. Waiter, J.H. Williams, A.D. Murray, A. Gilchrist, D.I. Perrett, A. Whiten, Structural white matter deficits in high-functioning individuals with autistic spectrum disorder: a voxel-based investigation, *Neuroimage* 24 (2005) 455–461.